Superstructure-foundation interaction in multi-objective pile group optimization considering settlement response

Y.F. Leung[1*], A. Klar[2], K. Soga[3], and N.A. Hoult[4]

[1]Department of Civil and Environmental Engineering, The Hong Kong Polytechnic University
[2]Faculty of Civil and Environmental Engineering, Technion–Israel Institute of Technology
[3]Department of Civil and Environmental Engineering, University of California, Berkeley
[4]Department of Civil Engineering, Queen's University

[*]Corresponding author, email address: andy.yf.leung@polyu.edu.hk

Abstract

The full potential of pile optimization has not been realized as the interactions between superstructures and foundations, and the relationships between material usage and foundation performance are rarely investigated. This paper introduces an analysis and optimization approach for pile group and piled raft foundations, which allows coupling of superstructure stiffness with the foundation model, through a condensed matrix representing the flexural characteristics of the superstructure. This coupled approach is implemented within a multi-objective optimization algorithm, capable of providing a series of optimized pile configurations at various amounts of material. The approach is illustrated through two case studies. The first case involves evaluation of the coupled superstructure-foundation analyses against field measurements of a piled raft-supported building in London, U.K. The potential benefits of pile optimization are also demonstrated through re-analyses of the foundation by the proposed optimization approach. In the second case, the effects of a soft storey on the superstructure-foundation interactions are investigated. These cases demonstrate the importance of properly considering the superstructure effects, especially when the building consists of stiff components such as concrete shear walls. The proposed approach also allows engineers to make informed decisions on the foundation design, depending on the specific project finances and performance requirements.

Keywords :Piled foundation, Superstructure stiffness, Matrix condensation method, Optimization analysis

Introduction

Foundation optimization presents opportunities to enhance engineering performance by accounting for specific project conditions, with potential savings in material consumption and costs. Earlier studies on the topic include Chow and Thevendran (1987), Truman and Hoback (1992), Horikoshi and Randolph (1998), Valliappan et al. (1999), Kim et al. (2001), Reul and Randolph (2004), and Leung et al. (2010b), etc. While the general features of optimal pile group designs have been discussed by some of these studies, it is difficult to derive an efficient technique to obtain optimum designs for various site conditions, considering the complexity of soil-pile interaction effects and potential stiffness contributions from the adjoining superstructure.

Due to the discrete nature of some design variables (e.g., number of piles and their locations), a mathematically continuous and differentiable function may not be formulated easily, and hence gradient-based optimization techniques are not always appropriate for such problems. To address this issue, Kim et al. (2002) applied an evolutionary algorithm, known as the Genetic Algorithm, to determine optimal pile locations in a piled raft design. Most evolutionary algorithms involve creation of an initial random population of candidate solutions (e.g. pile configurations), each evaluated by an objective function (e.g. foundation analysis model) which determines its survivability. The weak candidates (configurations that result in large settlements) are discarded and replaced by new members of the population, generated by combining the characteristics of 'strong' candidates. During this iterative process, the population gradually evolves based on the selection criteria. The application of evolutionary algorithms to foundation optimization has also been discussed by Ng et al. (2005), Chan et al. (2009), Hwang et al. (2011), Liu et al. (2012), etc. In this study, the significance of superstructure stiffness on foundation optimization will be investigated, while the relationship between material usage and optimal system performance will be revealed through multi-objective optimization analyses.

The optimization process is essentially driven by the objective function and selection criteria. For large pile groups, the critical design criteria are often associated with the differential settlements or distortions. Evaluations of such are significantly affected by features of the superstructure, yet the superstructure-foundation interactions are not rigorously considered in many pile group analyses, let alone their optimizations. Existing approaches to characterize such interactions include approximating the superstructure as beams with an equivalent stiffness (e.g. Meyerhof 1953; Sommer 1965) in the geotechnical model, or simulating the piles as 'spring constants' (e.g. Miyahara and Ergatoudis 1976) in the structure model. These, however, oversimplify the mechanism of interactions between superstructure, piles and the soil. Inaccurate modeling of such interaction effects in the objective function will also lead to unrealistic optimization results. Another common approach to evaluate the interactions involves iterative refinements of structural and geotechnical calculations (e.g. Chamecki 1956; Weigel et al. 1989). However, an iterative process increases the time and effort involved in a single foundation analysis, and the problem is exacerbated when optimization of pile layouts is required.

This paper introduces an analysis and optimization tool for piled foundations, which also enables efficient coupling of the superstructure stiffness. A multi-objective optimization technique is adopted to produce a series of optimized solutions at different amounts of material usage, thus providing the designer with a range of options according to the financial setup of the project. The analysis model (objective function) is first validated through a case study in London, U.K., where the potential benefits of foundation optimization are also demonstrated. A second case is then presented, which consists of a building with significant differences in stiffness across the storeys – a common practice for buildings with an atrium floor design. Through analyses of the two cases, this study will illustrate the importance of superstructure-foundation interaction in pile group modeling and optimization strategies. Preliminary studies on some of the components have been discussed in Leung et al. (2010a) and Leung et al. (2011), with illustrations on simple hypothetical scenarios. In the current study, however, the extended approach is evaluated with real building layouts, where the influence of various structural forms are discussed in detail.

Coupled superstructure-foundation modeling approach

Condensed superstructure stiffness matrix

The characteristics of the superstructure can play a crucial role in the overall structure and foundation performance (Small 2001; Poulos 2016), and the main objective of this study is to investigate such effects in pile optimization considerations. In the current study, the superstructure stiffness is incorporated into the piled raft foundation analyses through the matrix condensation method. In many building projects, structural engineers construct building models for design purposes using finite element packages. The complete structure model will consist of all the members in the building structure. Using these models, a 'condensed' structure matrix, denoted as $\mathbf{K}^s$ in the current work, can be generated by applying a unit displacement at each column in sequence, thus extracting the reaction forces at all other supports due to the unit displacement. For example, the component $\mathbf{K}^s_{i,j}$ in the condensed matrix represents the reaction force at support i due to a unit displacement applied at support j (Fig. 1a). Unlike the complete structural stiffness matrix, the condensed structure matrix is fully populated. For one degree of freedom, the size of condensed matrix will be $n \times n$, where n is the number of columns or supports connecting the superstructure and the foundation. In many cases, the superstructure may consist of continuous shear walls, and the associated

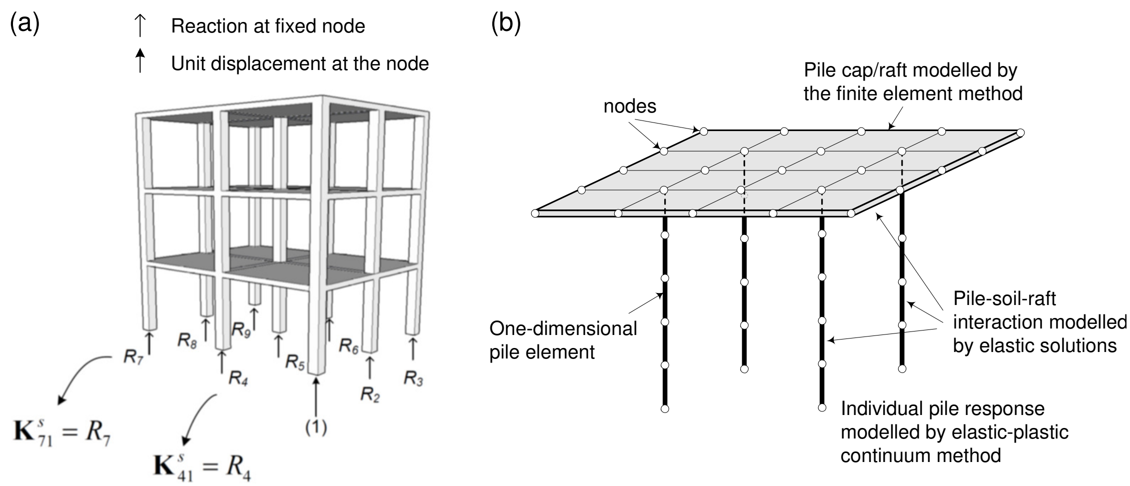

Figure 1: (a) Structure condensation process using finite element simulation, considering vertical load-settlement response (Leung et al. 2010a); (b) Schematic representation of piled raft model

$\mathbf{K}^s_{i,j}$ components can be obtained by incorporating a number of discrete supports along the wall in the finite element analyses. Poulos (1975) and Brown and Yu (1986) had discussed the formulation of such a matrix, but the subsequent analyses were focused on simple frame structures with assumptions of linear-elastic soil behavior. A similar sub-structuring technique had also been applied previously to replace the foundation by a condensed matrix, with the drawback of requiring an iterative solution process to account for nonlinear foundation response. In the current study, the matrix condensation method will be applied to represent the superstructure model, coupled with nonlinear analyses and optimizations of large pile groups and piled rafts.

The condensed structure matrix can be obtained by structural engineers using most structural finite element programs. To cover all load cases, the condensation process should also include horizontal and moment response (assuming the decision is made to detail the column-foundation connection to transfer moments), with a total of 6 degrees of freedom for each support (i.e. $6n \times 6n$ condensed matrix). This study will focus on the vertical load-settlement response with an $n \times n$ condensed matrix, while optimization of pile configurations will be performed to minimize vertical differential settlements. As the construction of structural finite element models has become increasingly common in building projects, the additional effort required to obtain the condensed matrix, which involves n analyses with prescribed unit displacements at the supports, is minimal. In fact, even if all 6 degrees of freedom are considered, the computational demands are not substantial, although manually handling the analysis may take more time before such operations are automated in commercial finite element programs. Meanwhile, coupling this condensed structure matrix into pile group analyses leads to more realistic modeling of the combined superstructure and foundation behavior, and eliminates the need for assumptions of Winkler spring constants or subgrade moduli, which cannot represent the behavior of soil continuum realistically.

A major assumption of the current approach is that the superstructure behaves in a linear-elastic manner. This is a more reasonable assumption in steel structures than in reinforced concrete buildings. However, this assumption is considered to be appropriate at working load levels for both steel and reinforced concrete buildings as the elastic modulus of concrete can be assumed to be linear at these levels. As will be discussed in later sections, the largest contribution to the stiffness comes from the shear walls, which will remain largely uncracked at working load levels, thus justifying the above assumption. Also, in a superstructure-foundation interaction problem, most of the nonlinearity will be contributed by the foundation response that arises from the nonlinear behavior at the soil-pile interface, and this will be discussed in the formulation of pile group analysis method in the next section.

It is worth noting that the actual superstructure stiffness changes as the building is being constructed. If the $\mathbf{K}^s$ matrix is developed based on the full building model, the foundation system will not experience its full stiffening effects when the building is still under construction. Meanwhile, the structural loads also increase with the construction process, leading to progressive changes in both load and stiffness that interact with the foundation. Brown and Yu (1986) stated that the interactions between a steel-framed structure and its raft foundation will be affected by assumptions of the loading sequence, i.e., whether the load is applied 'instantaneously' or 'progressively' in the model. In their settlement analyses, the discrepancies between the two models reduce as the raft becomes stiffer (increase in raft-to-soil stiffness ratio). The influence of loading sequence for a stiff structure on piled foundations will be assessed in a subsequent case study.

Pile group/piled raft analysis method

Fig. 1b shows the schematic diagram of the analysis model for pile groups and piled rafts. The raft (or pile cap) and the piles are discretised into segments specified by nodes, with the raft modelled as a thin plate using four-node rectangular elements. The nodal force vector and raft stiffness matrix are evaluated through the finite element method (Zienkiewicz and Taylor 2005). Interactions between the soil, raft and piles are evaluated based on elastic solutions, such as the Mindlin (1936) solution for homogeneous half space, or the Chan et al. (1974) solution for two-layered profiles, e.g., in cases where the bedrock is close to the pile tip level. Where the soil modulus increases linearly with depth ('Gibson soil'), the average Young's modulus of the two corresponding elements is used to evaluate the interaction effects, as suggested by Poulos (1979).

To model soil nonlinearity, a slip element (plastic slider) is incorporated into the continuum solution to limit the contact stresses between the soil and pile shafts and bases, and between the raft and the soil underneath. Formulation of this foundation analysis method has been described in detail by Leung et al. (2010b), and only the extensions to include superstructure effects are detailed herein. Considering the pile group/piled raft system, the soil-structure interaction can be described by:

$$(\mathbf{K}^p + \mathbf{K}^r)\, \boldsymbol{u} = \boldsymbol{p}^s + \boldsymbol{p}^g \tag{1}$$

where $\mathbf{K}^p$ is the structural stiffness matrix of the pile group, $\mathbf{K}^r$ is the raft stiffness matrix, $\boldsymbol{u}$ is the vector of raft and pile displacements at the nodes, $\boldsymbol{p}^s$ is the interaction force of the superstructure acting on the foundation, $\boldsymbol{p}^g$ is the ground reaction force acting on the pile and raft elements. For the superstructure to be in equilibrium, the following can be derived:

$$\mathbf{K}^s \boldsymbol{u} = \boldsymbol{p}^{fdn} + \boldsymbol{p}^w \tag{2}$$

where $\mathbf{K}^s$ is the condensed superstructure stiffness matrix mentioned earlier, $\boldsymbol{u}$ is the vector of column displacements, which is equal to the displacements at the corresponding foundation nodes connected to the columns. $\boldsymbol{p}^{fdn}$ is the interaction force of the foundation acting on the superstructure, and $\boldsymbol{p}^w$ is the loading due to the self-weight and live loads acting on the structure. It should be noted that the superstructure-foundation interaction forces are considered in $\boldsymbol{p}^{fdn}$, and therefore $\boldsymbol{p}^w$ represents the gravity loads assuming no interaction with the foundation (i.e. fixed foundations). This can be obtained from the support reactions assuming zero displacements at the supports in the superstructure model. Also, since $\boldsymbol{p}^s$ and $\boldsymbol{p}^{fdn}$ are action-reaction forces, they have equal magnitude but opposite signs:

$$\boldsymbol{p}^s = -\boldsymbol{p}^{fdn} = \boldsymbol{p}^w - \mathbf{K}^s \boldsymbol{u} \tag{3}$$

The reaction $\boldsymbol{p}^s$ can be interpreted as the superposition of two loads, one being the gravity load reactions using the fixed foundation system and the other being due to the differential settlements of the superstructure. It should be noted that $\mathbf{K}^s \boldsymbol{u}$ is only influenced by relative displacements between the supports, and is independent of the rigid body settlement of the whole structure. Substituting Eq. (3) into (1), and rearranging, results in:

$$(\mathbf{K}^p + \mathbf{K}^r + \mathbf{K}^s)\,\boldsymbol{u} = \boldsymbol{p}^w + \boldsymbol{p}^g \tag{4}$$

Eq. (4) is the governing equation of the coupled superstructure-foundation behavior. To model soil nonlinearity using slip elements, the procedures described in Leung et al. (2010b) are adopted, and Eq. (4) can be rewritten as:

$$\begin{aligned}
&(\mathbf{K}^p + \mathbf{K}^r + \mathbf{K}^s + \mathbf{K}^*)\,\boldsymbol{u} = \boldsymbol{p}^w + \mathbf{K}^*\boldsymbol{\lambda}^*\left\langle(\mathbf{K}^p + \mathbf{K}^r)\,\boldsymbol{u}\right\rangle + \mathbf{K}^*\boldsymbol{u}^{ip} \\
&\left\langle(\mathbf{K}^p + \mathbf{K}^r)\,\boldsymbol{u}\right\rangle_i = \min\left[(\mathbf{K}^p + \mathbf{K}^r)\,\boldsymbol{u}, f_{lim}\right]
\end{aligned} \tag{5}$$

where $\mathbf{K}^*$ is defined as the local soil stiffness matrix and is diagonal, $\boldsymbol{\lambda}^*$ is the soil flexibility matrix without the main diagonal, f_{lim} is the limit force at the raft and pile nodes, and $\boldsymbol{u}^{ip}$ represents the plastic interface displacements associated with the nodes. The soil-pile shaft contact force and soil-raft contact force are limited by different values of f_{lim}. Essentially, Eq. (5) introduces a plastic slider into the continuum solution, and an iterative procedure (Klar et al. 2007) is necessary to obtain the plastic displacements ($\boldsymbol{u}^{ip}$) at the soil-pile interface to represent the nonlinear foundation response. This elastic-plastic piled raft analysis approach (without considering the superstructure) has been shown to produce reasonable representations of nonlinear pile group and piled raft response (e.g. Poulos 1989; Guo and Randolph 1997; Leung et al. 2010c). It has also been validated against numerical analyses by Poulos et al. (1997) and several case histories in Europe (Katzenbach et al. 2000; Reul and Randolph 2003), details of which can be found in Leung (2010). In cases of complex subsurface stratigraphies, it is possible to incorporate the 'load transfer' approach into the current framework. This can be achieved by modifying the soil flexibility matrix in Eq. (5) using different nonlinear load transfer relationships for the associated soil layers.

Once the foundation settlements are determined, the corresponding settlements at column supports can be input into the superstructure model to obtain distribution of forces and moments in the structural members. This is different than most existing software packages that directly simulate the pile response as independent springs at column supports of the superstructure model, without considering the interaction effects among piles in the soil continuum. This drawback recently prompted Comodromos et al. (2016) to propose a method allowing for interaction among piles and the raft under combined loadings. The proposed approach in this study rigorously considers such pile-to-pile interaction effects, which can only be achieved otherwise by a complete three-dimensional finite element model consisting of the superstructure, foundation piles, and the entire soil domain. Meanwhile, the adopted coupling method allows a much faster simulation of all these components than the complete finite element model, and enables optimization analyses to be performed efficiently. In subsequent sections, this coupled superstructure-foundation analysis approach will be validated against measurements of a piled raft-supported building in London, U.K. Integration of this approach with optimization techniques will also be illustrated.

Multi-objective optimization algorithm

An efficient optimization algorithm can lead to savings in materials and improvements in foundation performance. Most previous studies on foundation optimization considered 'single-objective optimization', where the goal was either minimizing material costs under a tolerable performance level, or achieving the best performance with a certain amount of material (e.g. Kim et al. 2001; Chan et al. 2009). The two criteria in (minimizing) material usage and (maximizing) foundation performance were, however, not considered simultaneously. Also, the influence of superstructure was either ignored or grossly simplified in most previous works.

In the current study, the condensed superstructure stiffness ($\mathbf{K}^s$) is included into the foundation model. This becomes the objective function integrated into a multi-objective optimization algorithm, which is developed to obtain a range of optimized foundation solutions at different amounts of material usage. The technique is an extension of the Differential Evolution (DE) algorithm proposed by Storn and Price (1997) for search and optimization purposes, and is conceptually similar to other evolutionary algorithms. Besides demonstrating the potential benefits of foundation optimization, the study also aims to reveal the full stiffening effects of the superstructure as the holistic foundation-structure system performance is optimized.

Differential evolution

In the DE optimization process, a population of NP candidate solutions is first generated randomly. The candidate solutions are expressed as vectors of variables (known as trial vectors, $\boldsymbol{x}_i$) in the optimization problem. The algorithm then explores the search space by vector difference of the various candidate solutions. At each iteration (or 'generation'), 'mutant vectors' ($\boldsymbol{v}_i$) are formed by linear interpolation or extrapolation of trial vectors randomly selected from the population. A new generation of trial vectors ($\boldsymbol{y}_i$) is then formed by the 'crossover' process, whereby the components of mutant vectors are mixed with those of the trial vectors in the previous generation. The DE optimization process can be represented by the following equations (Storn and Price 1997):

$$\boldsymbol{v}_{i,G+1} = \boldsymbol{x}_{r1,G} + F(\boldsymbol{x}_{r2,G} - \boldsymbol{x}_{r3,G}) \tag{6}$$

where $\boldsymbol{v}_{i,G+1}$ is the mutant vector in generation $G+1$, formed by interpolation of three randomly selected trial vectors from the previous generation G. F is an amplication factor of the differential variation between two trial vectors $\boldsymbol{x}_{r2,G}$ and $\boldsymbol{x}_{r3,G}$. The crossover process is then represented by:

$$\begin{aligned} \boldsymbol{y}_{i,G+1} &= \{y_{1i,G+1}, y_{2i,G+1}, \dots, y_{Di,G+1}\}^T \\ y_{ji,G+1} &= \begin{cases} v_{ji,G+1} & \text{if } randb(j) \leq CR \text{ or } j = rnbr(i) \\ x_{ji,G} & \text{if } randb(j) > CR \text{ and } j \neq rnbr(i) \end{cases}, j = 1, 2, \dots, D \end{aligned} \tag{7}$$

where $y_{ji,G+1}$ is the j^{th} component of the new trial vector, which, like $\boldsymbol{x}_i$ and $\boldsymbol{v}_i$, has D components. CR is a crossover constant chosen by the user and $randb(j)$ are random numbers to be compared with CR to decide values of $y_{ji,G+1}$. Another random index, $rnbr(i)$, which is a random integer between 1 to D, is introduced to ensure $\boldsymbol{y}_{i,G+1}$ has at least one component of $\boldsymbol{v}_{i,G+1}$.

Fitness of $\boldsymbol{x}_{i,G}$ (parent, in generation G) and $\boldsymbol{y}_{i,G+1}$ (child, in generation $G+1$) are evaluated and compared through an objective function, which is the coupled superstructure-foundation analysis in the current study. The fitness (e.g., foundation settlement) determines the survivability of the particular solution – the fitter solutions stay in the population, while the weaker ones will be discarded. The comparisons are performed for each parent-child pair (i from 1 to NP), and the procedures are iterated until the population converges to a global optimum solution.

Pareto Optimality

It is a common perception that reducing material usage and improving foundation performance are two conflicting design criteria: more foundation material often leads to better overall foundation performance, but this is limited by the financial implications and environmental impacts associated with increased material consumption. Currently, this decision-making process relies mainly on experience of individual practitioners. In fact, it can be handled analytically using a multi-objective optimization technique, i.e.,

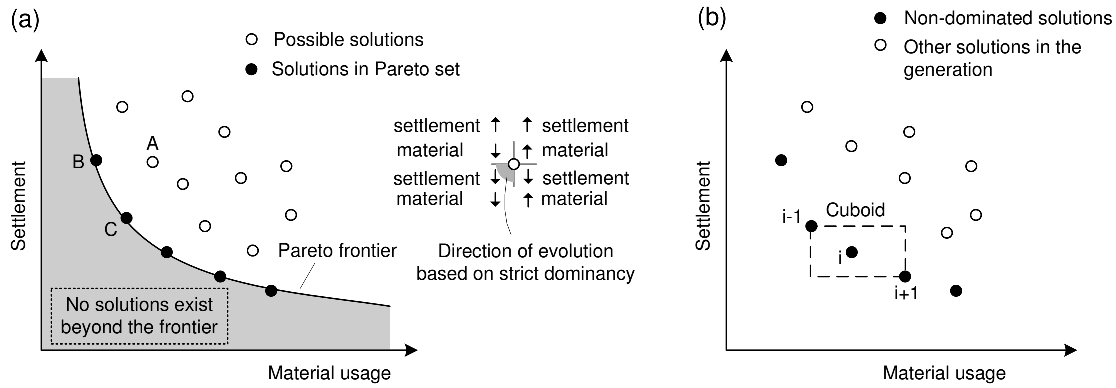

Figure 2: (a) Concept of Pareto optimality in foundation optimization; (b) Calculation of crowding distance (after Deb et al., 2002)

to obtain the least amount of material required to achieve a certain level of performance, meanwhile ensuring the foundation material is arranged in an optimized manner.

In the current study, the DE is implemented under a multi-objective optimization framework based on the concept of Pareto optimality (Fig. 2a) (Reddy and Kumar 2007; Lavan and Dargush 2009). Under this framework, a 'Pareto frontier' is defined as an optimized relationship between the objectives of optimization (e.g., foundation cost and foundation settlements) where no further improvement can be made for one criterion without worsening the other. This means, in the context of foundation optimization, that no configuration can exist 'beyond' the Pareto frontier, with both a smaller amount of material usage and a better performance compared to configurations on the frontier.

In multi-objective foundation optimization, the aim of DE is to obtain the Pareto frontier, which is an initially unknown relationship of optimized material usage and foundation performance. In this case, a fitter solution is defined as the one that is not worse in any objectives, and better in at least one objective, compared to another solution. This condition is known as 'strict dominancy'. As illustrated in Fig. 2a, Solution A is strictly dominated by both Solutions B and C, since both B and C have at least one criterion better (smaller settlement/material usage) than A, and are not worse than A in the other criterion. Solutions B and C are not strictly dominated by each other, since B involves less material and C leads to smaller settlements. This is also the case for all solutions on the Pareto frontier. Incorporating this concept into the context of DE, a trial vector replaces another if it strictly dominates the other trial vector. Consequently, an initial random population (empty circles in Fig. 2a) will gradually 'march' towards, and eventually converge on, the Pareto frontier as they evolve in subsequent generations.

Elitist non-dominated sorting

In typical 'single-objective' evolutionary algorithms, a 'child' vector is only compared with its own 'parent' vector (i.e. $\boldsymbol{y}_i$ with $\boldsymbol{x}_i$ at the same i). Consequently, some good solutions may be lost in the process if they are better than many other solutions but weaker than its own parent. This issue is more prominent in multi-objective optimization problems, as $\boldsymbol{y}_i$ can be strong in one criterion but is eventually discarded for being slightly weaker than $\boldsymbol{x}_i$ in another criterion. To preserve these 'good' solutions and hence speed up the optimization process, the idea of the non-dominated elitist archive (Deb et al. 2002; Reddy and Kumar 2007) is adopted in the current study. This archive is essentially a list of the best non-dominated solutions in the current generation, and allows comparisons among all the trial vectors (i.e. all $\boldsymbol{y}_i$ and $\boldsymbol{x}_i$ where $i = 1, 2, \ldots, NP$) in the previous and current generations. The process may be interpreted as the evolution of the entire frontier, instead of individual candidates, in each generation.

In addition, due to the random nature of DE, the resulting Pareto set may lack a desirable spread of solutions along the frontier, with solutions being 'crowded' in some regions but few and far between in others. To obtain a good spread of solutions in the generation, a 'crowding distance' is evaluated for each solution in the archive generation (Fig. 2b) (Deb et al. 2002). The crowding distance of solution i is defined as the average side length of the cuboid formed by the two adjacent solutions ($i-1$ and $i+1$). In case the size of the non-dominant archive becomes bigger than the population size, the final population will be decided based on the crowding distance of each individual solution, and those with a large crowding distance are preferred. This helps to enhance representation of the Pareto set and improve the efficiency of multi-objective optimization.

Case study of Hyde Park Cavalry Barracks, London

The Hyde Park Cavalry Barracks (HPCB) Tower in London, U.K., will be used to evaluate the coupled superstructure-foundation analysis approach, and to illustrate the capabilities of the optimization technique. The foundation geometry, underlying soil conditions, instrumentation setup and back analyses for the piled raft foundation have been reported extensively by Hooper (1973, 1979). In addition, superstructure plans and section sizes have been described in detail. Such information enables the modeling of the foundation, taking into account the effects of superstructure stiffness.

Details of superstructure, foundation and soil properties

The HPCB tower is 90 m tall with a two-storey basement. The tower is founded on a 1.52-m thick raft supported by 51 under-reamed piles, each with a length of 24.8 m, shaft diameter of 0.91 m and base diameter of 2.44 m. Fig. 3a shows the actual foundation layout, where the shaded area represents the plan area of the raft that is in contact with the soil. The subsurface soil profile consists of 5 m of fill, sand and gravel, followed by a 58-m thick layer of London Clay. The London Clay is underlain by the Lambeth Group with a thickness of approximately 21 m, which is in turn underlain by a thin layer of Thanet sand and Chalk bedrock. The groundwater level was approximately 4 m below

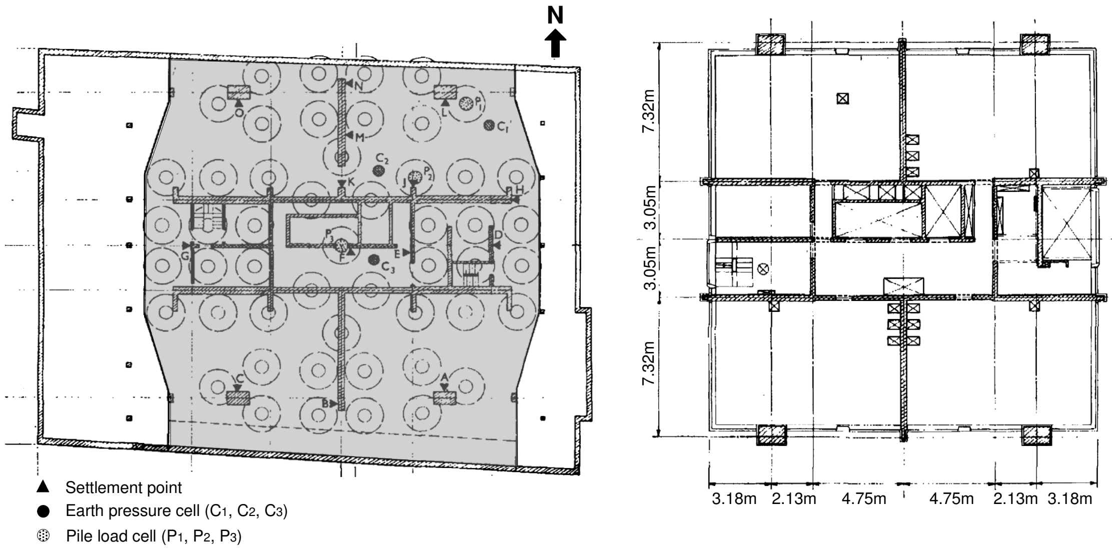

Figure 3: Foundation and superstructure layout of Hyde Park Cavalry Barracks (Hooper 1973)

the ground surface. For modeling purposes, it is assumed in the subsequent analyses that properties of the Lambeth Group are not significantly different from those of the London Clay.

The concrete tower consists of 31 storeys and the typical structural floor plan is shown in Fig. 3b. The thicknesses of core walls are 381 mm and 457 mm up to the second floor, 229 mm and 381 mm between the third and ninth floors, and 229 mm and 305 mm on and above the tenth floor. The floor slabs are 178 mm thick, supported on the inner side by the core walls, and on the outer side by edge beams that are 1070 mm deep and 152 mm thick. The main tower columns are 1520 mm by 915 mm. The top floor and roof are believed to have a different layout. Their exact layout is, however, not reported in the literature and therefore the floor plans are assumed to be constant throughout. Sensitivity analyses have been conducted by varying the layout and section sizes of the top two floors, and they only have a minimal impact on the overall foundation behavior.

The properties of London Clay are essential for foundation modeling as the piled raft is entirely embedded in this type of soil. Based on the soil test data reported in

Hooper (1973), Eq. (8) is derived to represent the increase of undrained shear strength (in kPa) with depth (in metres):

$$s_u = 100 + 11z_{clay} \tag{8}$$

where z_{clay} is the depth measured from top of the clay surface, which is approximately 5 m below ground surface. The pile shaft resistance was estimated using the total stress approach (α-method), adopting $\alpha = 0.5$. The shaft resistance estimated by the total stress method and the effective stress method (assuming typical London Clay parameters) are similar to each other, and the α-method is adopted as it is based on *in-situ* measurements of s_u. Meanwhile, based on previously published data and results of back-analyses, Hooper (1973) proposed the following relationship between the drained and undrained Young's moduli (E' and E_u) of the London Clay (in MPa) and the corresponding depth:

$$E' = 0.75E_u = 0.75(10 + 5.2z) \tag{9}$$

where z is the depth (in metres) measured from the ground surface. The factor 0.75 corresponds to a drained Poisson's ratio of 0.1. The shear modulus can then be estimated for evaluation of interaction effects between the soil, pile and raft elements ($\mathbf{K}^*$ and $\boldsymbol{\lambda}^*$ in Eq. (5)), using the Chan et al. (1974) solution with Chalk layer taken as the firm stratum.

Validation of piled raft analysis incorporating superstructure stiffness

Hooper (1973) adopted an 'equivalent raft thickness' (t_e) of 3.3 m in his back analyses to simulate the stiffening effects of the superstructure. This is more than 100% larger than the actual thickness of the raft (1.52 m). In the current study, the matrix condensation method is applied for more realistic foundation analyses and subsequent optimization.

The superstructure is modelled using LUSAS, which is a commercial finite element software package. The condensed structural matrix ($\mathbf{K}^s$) is then obtained through procedures described earlier (Fig. 1), assuming a long-term concrete Young's modulus of 14 GPa, which takes into consideration the creep behavior of concrete. The value of long-term concrete modulus is recommended by the LUSAS program, and agrees with the estimates based on Eurocode 2 (British Standards Institution 2008).

According to Hooper (1973), the estimated total weight of the structure, including dead and live loads, is 228 MN, which matches the estimates from the structural finite element model when gravity loads of 3 kPa (including live loads and floor finishes) are applied on all the floor slabs. Line loads of 2 kN/m are imposed on the outer edge beams to simulate the weight of the façade including precast concrete elements and window panes. The column and wall reactions ($\boldsymbol{p}^w$) arising from these loads are applied as downward vertical loads, while the unloading due to excavation for basement construction, minus the weight of the foundation raft, is applied as an uplift pressure.

Fig. 4a shows an encouraging agreement between measured settlements and analyses with $\mathbf{K}^s$ incorporated. The settlement at the raft center is predicted to be 23.5 mm by the analyses, while the measured center settlement was 21 mm. The estimated differential settlements range from 5–6.5 mm in various directions, while the measured values were between 3.5–6.5 mm. On the other hand, analyses without considering superstructure effects overestimate the differential settlements of the foundation (>10 mm), in some cases by more than 100%. This would lead to overestimating the distortion and potential cracking in the structure, or may lead the designers to adopt unnecessarily thick rafts resulting in increases in material use and cost. For example, the equivalent raft thickness ($t_e = 3.3$ m) adopted by Hooper (1973) was based on two-dimensional, axisymmetric finite element analyses, to represent a tenfold increase in raft bending stiffness compared to the actual raft thickness. Alternatively, using the piled raft analysis model in

Table 1: Comparisons between results of staged and 'instantaneous' construction models of HPCB tower

	Staged construction	'Instantaneous' construction
Center settlement (mm)	23.3	23.4
Differential settlement (N-S)(mm)	5.1	5.1
Differential settlement (E-W)(mm)	5.2	5.2
Differential settlement (diagonal)(mm)	6.7	6.6
Maximum differential settlement (mm)	14.6	14.5

this study, sensitivity analyses are performed by increasing the raft thickness without incorporating $\mathbf{K}^s$. Fig. 4b shows the results of this sensitivity study, where the settlement measurements can be matched by adopting t_e of 2 m. This represents a 32% increase compared to the actual raft thickness.

The previous analyses are performed with the assumption that the complete superstructure stiffness and loads are imposed onto the foundation 'instantaneously'. To investigate the effects of progressive loading on foundation settlements described by Brown and Yu (1986), a stepwise analysis was also performed where three construction stages are considered – at 10 storeys, 20 storeys, and completion of building. For each stage, the corresponding structure models are constructed to obtain the associated $\mathbf{K}^s$ matrix and $\boldsymbol{p}^w$ vector, and the incremental displacements ($\boldsymbol{u}$ and $\boldsymbol{u}^{ip}$) are then solved according to Eq. (5). Table 1 compares the final settlement estimates from the 'instantaneous' and 'staged' load assumptions, and shows that the settlement values are almost identical. To reduce computational effort, the subsequent optimization analyses are therefore performed with the assumption of instantaneous loading as the main selection criterion is the differential settlements in the foundation.

Fig. 5 shows the comparison between the measured pile loads and predictions by the current analyses. Pile force estimates (incorporating $\mathbf{K}^s$) for piles P1, P2 and

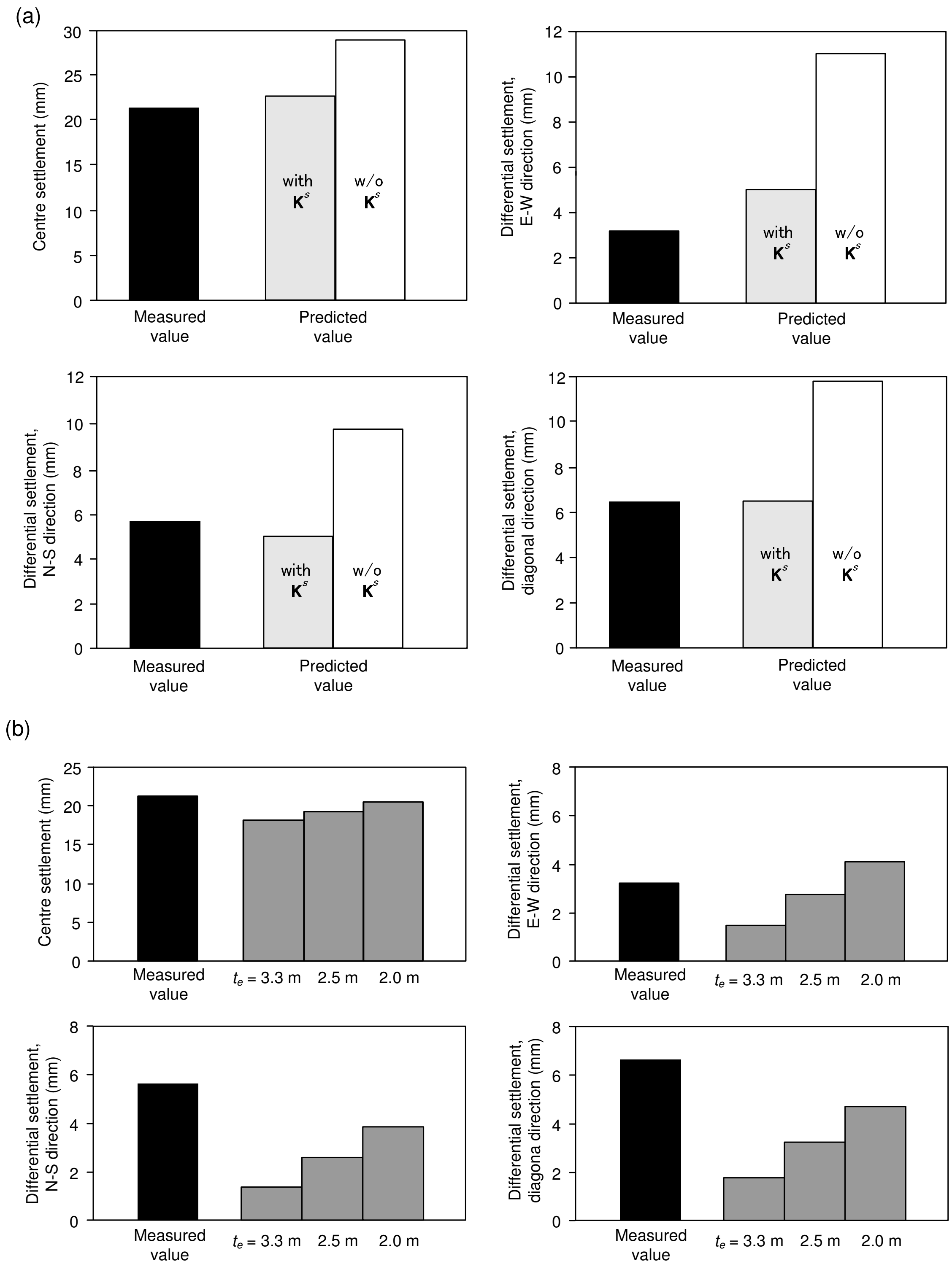

Figure 4: (a) Comparisons of settlement estimates for Hyde Park Cavalry Barracks; (b) Sensitivity analyses with different equivalent raft thickness ($\mathbf{K}^s$ not incorporated)

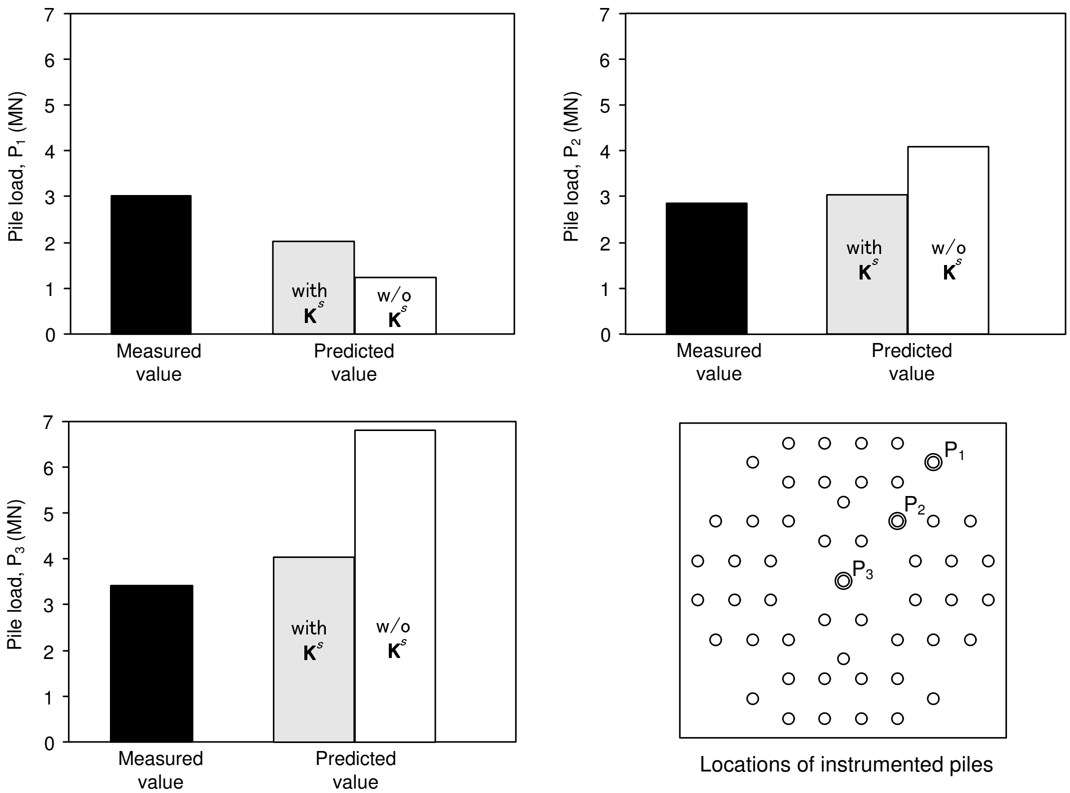

Figure 5: Comparisons of pile force estimates for Hyde Park Cavalry Barracks

P3 range from about 2000 kN to 4100 kN, while the measured forces were between 2850 kN to 3400 kN. The maximum discrepancy between the estimated and measured values is approximately 30% (pile P1). On the other hand, without including $\mathbf{K}^s$, the discrepancies for pile force estimates range from 44% to over 100% for the three piles. The improvements obtained through incorporating $\mathbf{K}^s$ are significant, as the building stiffness also affects the distribution of loads onto the foundation system.

Optimization of HPCB foundation

The case study of HPCB foundation can also be used to illustrate the multi-objective optimization approach, with $\mathbf{K}^s$ incorporated into the foundation analyses. Coding the foundation configuration as trial vectors is a key aspect in DE. This is shown in Fig. 6, which outlines the scheme to optimize both the pile lengths and pile locations for the

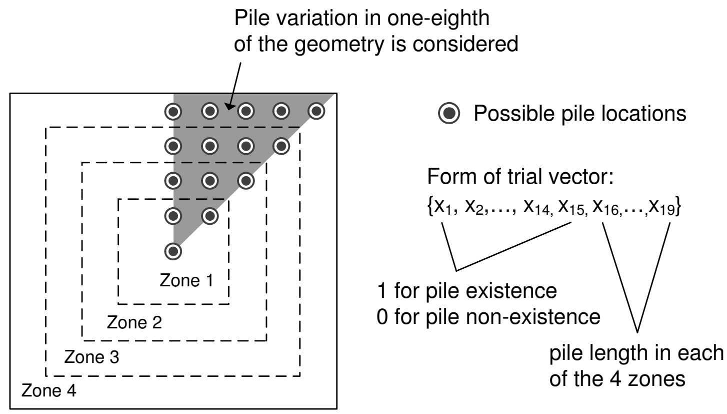

Figure 6: Optimization scheme for piled raft of Hyde Park Cavalry Barracks

HPCB piled raft. The scheme takes advantage of piled raft symmetry and imposes uniform pile lengths at similar distances from the center. As illustrated by the shaded area in Fig. 6, a trial vector represents the variations of pile geometry in one-eighth of the foundation geometry, and the variations are imposed to the entire foundation to ensure symmetric conditions. For the HPCB foundation, the trial vector consists of 15 possible pile locations. Each of the first 15 components (position components) of the trial vector is equal to either 1 or 0, and determines the existence or non-existence of piles in each of the 15 locations. The second part of the vector (length components), consisting of 4 components in this case, controls the pile lengths in each of the 4 zones at different distances from the center of the raft. The length of trial vector, D, is therefore 19 in this case.

In the current study, the selection criterion in the DE algorithm is to minimize the differential settlement, defined herein as the difference between the maximum and minimum settlements across the raft. Depending on specific project conditions, other criteria may be applicable. Examples of these could include the rocking movements and horizontal deflections due to wind loads on very tall buildings, which will result in different optimized pile configurations. The purpose of the following analyses is to demonstrate the capabilities of the proposed technique under a certain selection criterion, which is the differential settlement under vertical loads.

To ensure realistic pile configurations in the optimization, the numbers of piles are allowed to vary between 45 to 55, and the maximum ratio between the longest and shortest pile lengths is 1.5. The pile diameter is assigned to be 0.91 m, which is the same as the original configuration. Optimization analysis is then performed with a population size (NP) of 100.

Multi-objective optimization places a high demand on computing power due to the large number of possible pile configurations with varying amounts of material. Therefore, a two-stage optimization approach has been adopted. The Pareto frontier is first developed using linear-elastic piled raft analyses, where the large number of potential pile configurations is evaluated using relatively fast elastic analyses. In the second stage, the frontier is refined by subjecting the solutions on the 'elastic' frontier to more rigorous elastic-plastic analyses.

Fig. 7 shows the Pareto frontier developed by this two-stage optimization approach. Fig. 7a shows the first stage using the elastic analyses, whereas the solid circles in Fig. 7b are the Pareto frontier refined by the second stage, using elastic-plastic analyses. The process of evolution towards the frontier is revealed by the distribution of solutions in the 10^{th}, 20^{th} and 50^{th} generations, as shown in Fig. 7a. The analysis is terminated at the 50^{th} generation as a stable frontier has developed, and the resulting configurations are subjected to elastic-plastic analyses, leading to the refined frontier shown in Fig. 7b (solid circles). Average settlements of several configurations on the frontier are also shown in Fig. 7b as they can be important concerns in the design. For verification purposes, optimization with elastic-plastic analyses, which should result in the true frontier, is also performed for comparison, using a smaller NP of 30 to reduce the required computational effort. This frontier is shown by empty circles in Fig. 7b. Not only do

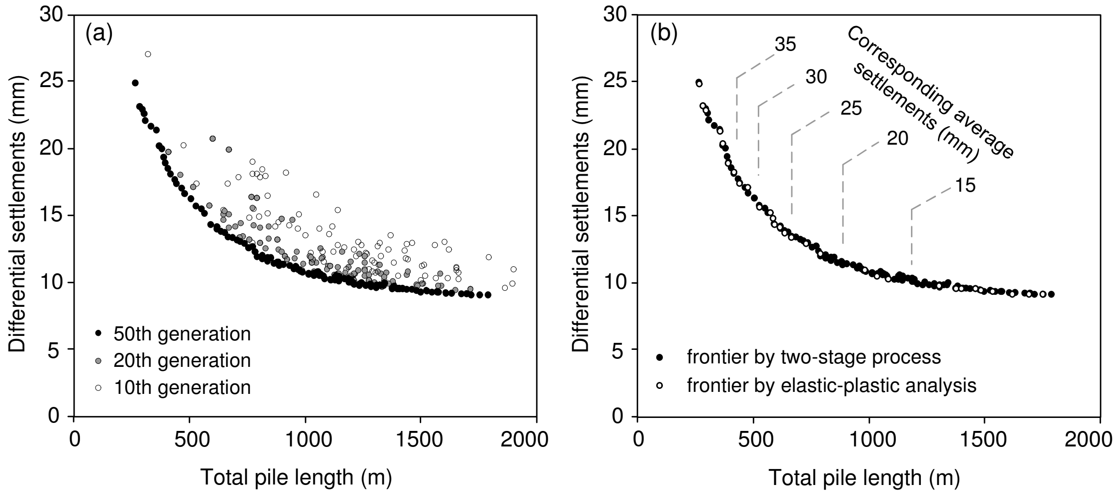

Figure 7: (a) Development of Pareto frontier using the two stage process; (b) Refined Pareto frontier with elastic-plastic analyses

the two frontiers coincide with each other, the geometries of optimized configurations obtained from the two sets of analyses are also very similar.

The two-stage process involves optimization using elastic analyses, refined by elastic-plastic analyses on the final Pareto set. In theory, the frontier developed by elastic analyses (Stage 1) is the lower bound of the true relationship since elastic analyses always result in displacements smaller than or equal to those predicted by nonlinear analyses. On the other hand, the refined frontier developed at Stage 2 represents the upper bound of the true frontier. This is because if the true frontier consists of 'fitter' configurations than the refined frontier, they must result in smaller displacements than those in the two-stage process. In the case of HPCB Tower foundation, the frontier developed by the two-stage process (Fig. 7a) is almost identical to the refined frontier (Fig. 7b). This is mainly because the raft alone provides sufficient resistance to resist the structural loads, while the piles are installed mainly to control settlements. The overall margin of capacity provided by the piled raft is large - hence the degree of nonlinearity is low - resulting in similar predictions of displacements by elastic and elastic-plastic analyses.

Discussions on optimized pile configurations

The Pareto frontier entails optimized pile configurations with different amounts of material usage, represented in this case by the sum of lengths (or total lengths) of all piles in the piled raft. A closer examination of these configurations reveals that they share similar general characteristics. For example, Fig. 8 shows the optimized configurations with total lengths of all piles being 500 m (Fig. 8a), 1250 m (Fig. 8b) and 1500 m (Fig. 8c). All these configurations consist of piles directly underneath the heavily-loaded shear walls of the tower (Fig. 3). In general, longer piles are located close to the central part of the raft while shorter piles are placed near the periphery to reduce differential settlements. The features of these configurations also match with the general recommendations by Leung et al. (2010b) and Reul and Randolph (2004), who stated that considering the same total pile length, using small numbers of long piles is more effective in reducing settlements, and differential settlements are efficiently reduced by installing piles under the central area of the foundation.

The original pile configuration (Fig. 3) involves a total pile length of about 1250 m, resulting in differential settlement of 14.5 mm. According to Fig. 8b, the optimized layout with 1250 m of pile material results in differential settlement of only 10 mm, which represents a 30% reduction. On the other hand, for a required performance level of 14.5 mm in differential settlements, it is possible to reduce the total pile material to 650 m according to the Pareto frontier (Fig. 7), which represents a reduction of approximately 50% in pile material.

Apart from foundation settlements, the pile forces and bending moments induced in the raft are also evaluated by the proposed approach. Fig. 9 compares bending moments evaluated based on the original pile configuration (Fig. 3a) and the optimized configu-

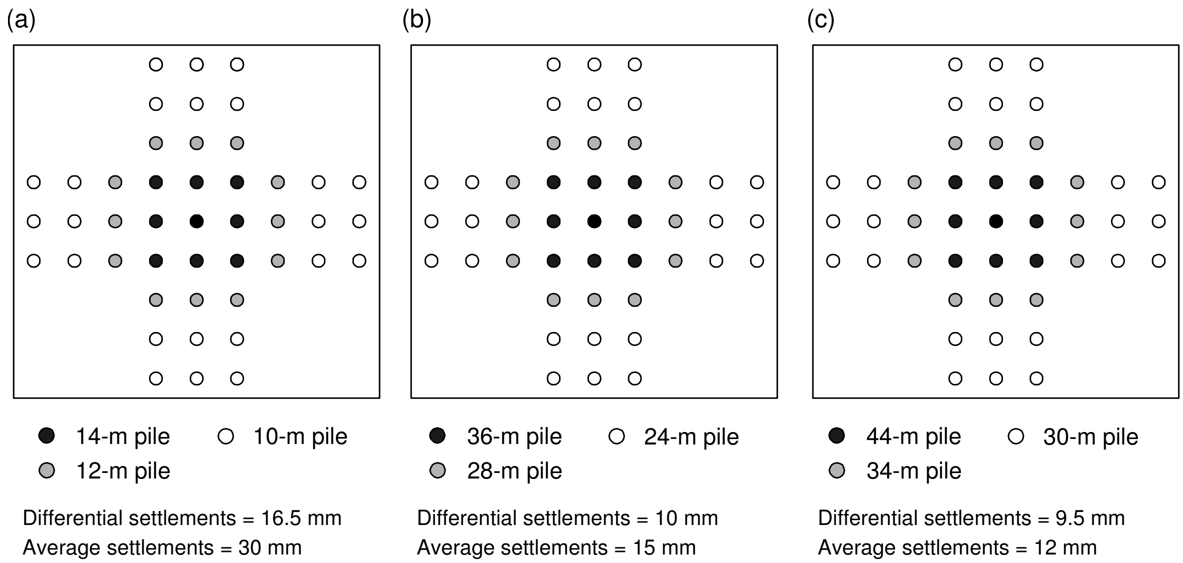

Figure 8: Optimized pile configurations with different total pile lengths of (a) 500 m; (b) 1250 m; (c) 1500 m. Original configuration involves total pile length of 1250 m, average settlement of 17 mm and differential settlement of 14.5 mm

ration, with total pile length of 1250 m (Fig. 8b). Under the optimized configuration, the bending moments are reduced in the central area of the raft, but there are slight increases near the raft edges, as it consists of fewer piles near the edge columns of the structure than the original configuration.

Fig. 10 compares the maximum and minimum pile forces in the original and optimized piled raft configurations (Fig. 8b), and shows that the range of pile force variation has not been significantly altered in the optimized configuration. In the current optimization scheme, the maximum ratio between the longest and shortest pile lengths is 1.5. The rationale behind this limit is to avoid 'ultra-long' piles in the foundation, which tend to attract more load than other piles, and where defects or underperformance of such elements can be more detrimental. Over-reliance on certain long piles can undermine the redundancy of a foundation system as the overall reliability hinges on the behavior of a few very stiff elements. The maximum/minimum pile length ratio of 1.5 helps to ensure redundancy in the foundation design is not compromised in the optimized configuration.

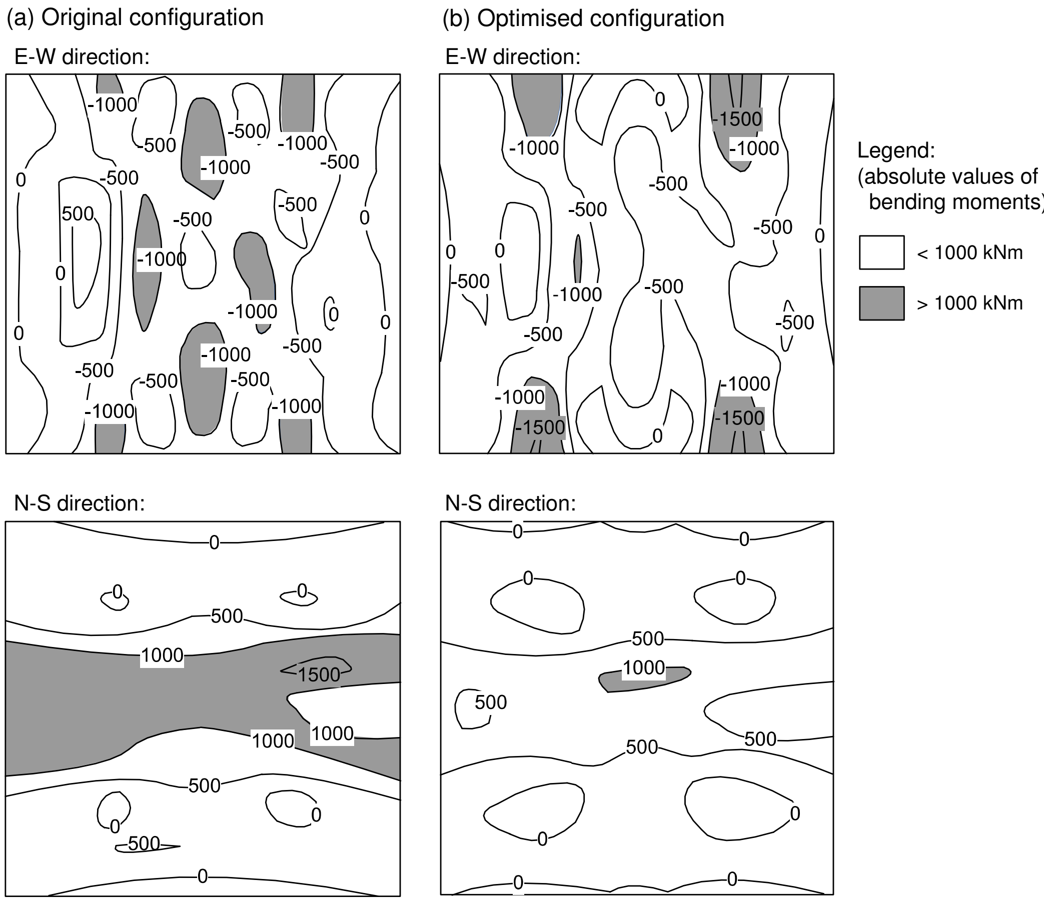

Figure 9: Bending moment estimates for (a) original pile configuration and (b) optimized pile configuration with total pile length of 1250 m

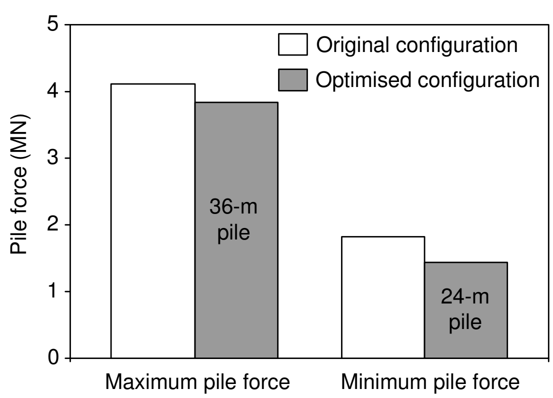

Figure 10: Comparisons of maximum and minimum pile forces between original and optimized pile configurations for HPCB tower

Case study of building with soft storey on ground floor

The HPCB building consists of floor layouts that remain relatively constant throughout the height of the building, although the shear wall thickness varies slightly on different storeys. However, in order to create open space on the ground floor, it is not uncommon for buildings to incorporate an atrium floor that is significantly less stiff than the upper storeys. This abrupt change in floor layout may influence how the superstructure stiffness is transferred to the foundation system.

Fig. 11 shows the floor plans simplified from a typical residential block in Hong Kong, China, which is a 25-storey reinforced concrete building with an atrium on the ground floor and 24 typical upper floors. The atrium floor consists of 12 columns with dimensions ranging from 762 mm$\times$ 1219 mm to 762 mm$\times$ 1829 mm. From the second storey upward, the floor layout consists of concrete walls with thickness of 152 mm. Apart from the 4-m high atrium, each storey is 3 m in height, with floor slab thickness varying from 102 mm to 127 mm in different areas of each floor. The atrium and upper floors are connected by deep transfer beams with section sizes ranging from 381 mm $\times$ 1219 mm (width $\times$ depth) to 889 mm $\times$ 2565 mm. To illustrate the significance of the open atrium, a second building model is created without the atrium for comparison purposes. This building consists of 25 storeys of the same floor plan as shown in Fig. 11a. The first storey is 4 m high while the upper floors are all 3 m in height. Besides the self weights of structural components, 5 kPa of superimposed dead load and live loads are modelled, and the $\mathbf{K}^s$ matrix and $\boldsymbol{p}^w$ vector for each building are obtained using the procedures described earlier.

The two buildings are assumed to be founded on piled rafts, and the soil conditions for this hypothetical case consist of a homogeneous soil layer with $E' = 40$ MPa and Poisson's ratio of 0.3. The pile capacities are evaluated using the effective stress approach,

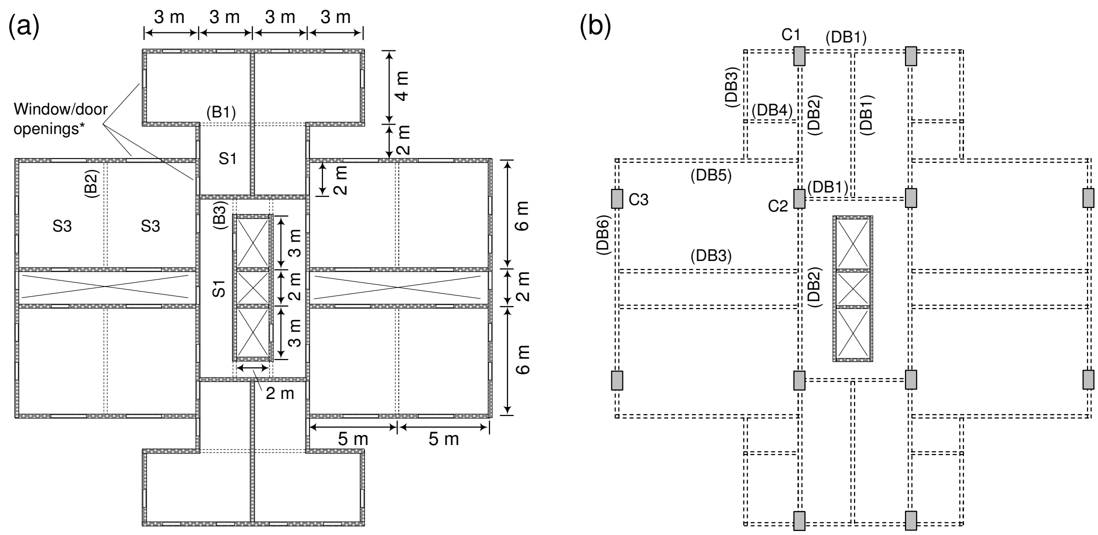

Dimensions of slabs (S), beams (B, DB) and columns (C):

S1: 102 mm (thickness)
S2: 114 mm (thickness)
S3: 127 mm (thickness)

B1: 152 mm x 457 mm
B2: 305 mm x 457 mm
B3: 152 mm x 381 mm

C1: 762 mm x 1219 mm
C2: 762 mm x 1829 mm
C3: 889 mm x 1295 mm

DB1: 610 mm x 2565 mm
DB2: 762 mm x 2565 mm
DB3: 457 mm x 2565 mm
DB4: 381 mm x 1219 mm
DB5: 686 mm x 2565 mm
DB6: 889 mm x 2565 mm

*Windows are modelled as 1 m x 1 m or 2 m x 1 m openings, while doors are modelled as 2 m x 1 m openings

Figure 11: Superstructure layout for hypothetical building: (a) typical floor; (b) atrium floor. Building is symmetrical in two directions

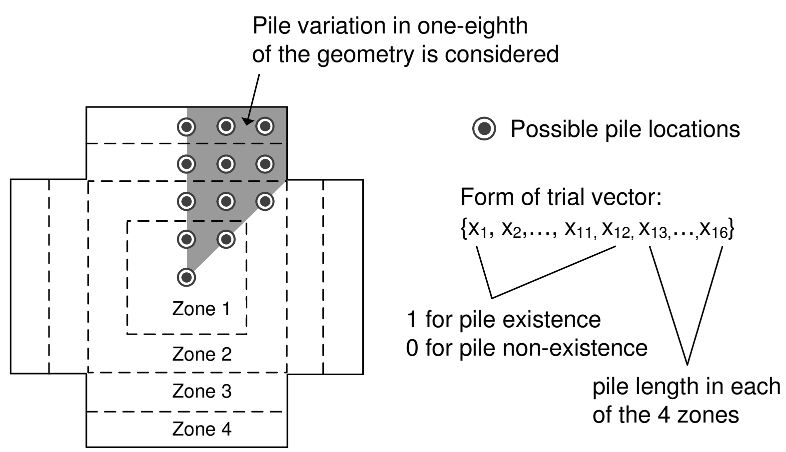

Figure 12: Optimization scheme for piled raft of hypothetical building

assuming a friction angle of 32° and shaft resistance coefficient of 0.5. The water table is assumed to be at the base of a 1.5-m thick raft.

As shown in Fig. 12, the raft is modelled with a cruciform shape to match the superstructure layout, while the pile optimization scheme is derived to take advantage of the symmetry conditions. The trial vector consists of 16 components, where the first 12 determine pile locations and the remaining 4 decide the pile lengths at various zones. The pile diameter is taken as 0.9 m, the number of piles is allowed to vary from 40 to 55, and the maximum length ratio is 1.5 as in the HPCB case.

Influence of atrium floor on foundation optimization

Multi-objective optimization analyses are performed for the two buildings, one with the atrium design at ground floor level and the other one with constant floor stiffness and no atrium. For both optimization analyses, the population size (NP) is 100, and the two-stage approach is adopted with Pareto frontiers first developed using linear-elastic analyses, and then refined by elastic-plastic analyses. Fig. 13a shows the Pareto frontiers for the optimized piled raft foundations supporting the two different buildings. Although the two superstructures only differ by the first storey, the difference in the performance of the optimized foundations is notable. For example, with the material usage of approximately 400 m in total pile length, the optimized pile configuration leads to differential settlements of 6 mm for the building with an atrium, and only about 3 mm for the building with shear walls on the first storey and no atrium. In other words, the presence of an atrium floor reduces the stiffening effects of the superstructure, as the stiffness of shear walls on upper storeys is not effectively transferred to the foundation.

Considering the same pile configurations, Fig. 13a also shows the corresponding analyses when the superstructure stiffness ($\mathbf{K}^s$) is not coupled with the foundation model. For both cases, the differential settlements are larger when $\mathbf{K}^s$ is not considered.

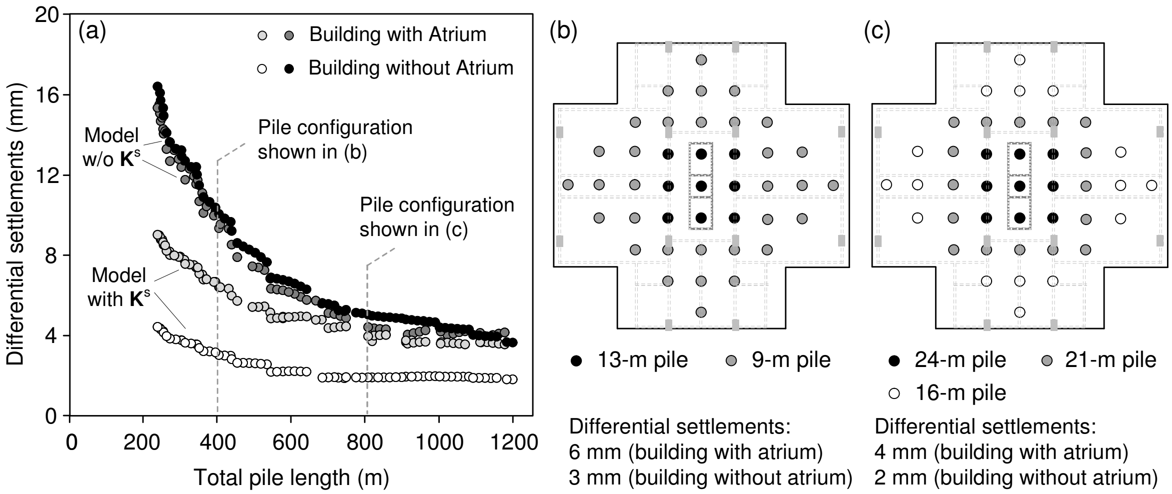

Figure 13: Pareto frontiers and optimized pile configurations for buildings with and without atrium floor

As the superstructure and foundation behave in a holistic manner, the importance of $\mathbf{K}^s$ also depends on the stiffness of the foundation system. The stiffening effects of the superstructure are more substantial when small amounts of pile material are used, and gradually diminishes as the pile length increases, i.e., when stiffer foundations are installed. In most cases, however, the influence of $\mathbf{K}^s$ should not be overlooked. For example, with the building geometry shown in Fig. 11, differential settlements of about 13 mm correspond to a deflection ratio of 0.05%. If this is adopted as the allowable limit for the structure, analyses without including $\mathbf{K}^s$ could lead the engineer to increase the number of piles or the thickness of raft in the foundation design. This again highlights the importance of realistic modeling of superstructure-foundation interactions for pile group/piled raft analysis and optimization. Two examples of the optimized pile configurations are shown in Figs. 13b and c. Although optimization analyses are performed separately for the two buildings, the resulting optimized pile configurations are identical at most cases of material usage. This may be attributed to the fact that load distributions across the foundations are similar between the two buildings. The 24 typical upper storeys involve the same floor layout and load patterns for both buildings. Although such loadings are carried by columns at the atrium floor, and by walls for the building without the atrium, they eventually lead to similar load distribution on the raft and hence the same optimized pile configurations. Similar to the HPCB case, the optimized configurations involve long piles near the center of the foundation and shorter piles around the periphery, which is typical when the optimization criterion involves minimizing differential settlements under vertical loads.

Conclusion

This paper introduces the matrix condensation method which allows coupling of superstructure stiffness into pile group and piled raft foundation models. This approach forms a link between the structural and geotechnical engineers, through which accurate global solutions can be obtained without the need for relaxing assumptions on the contribution of superstructure to the foundation system, and vice-versa.

Considerations of the superstructure stiffness and load distribution can play an important role in the foundation optimization process, especially when structural elements such as shear walls contribute significantly to the settlement response of piled foundations. In the current study, the coupled analysis approach is incorporated into a multi-objective pile optimization algorithm, which provides a series of design options at various levels of material consumption, with each design option representing the optimized configuration using that particular amount of pile material. This reveals the trade-off between material usage and foundation performance, and can help engineers make informed decisions on the design based on its cost-effectiveness and the performance requirements. While many engineers currently rely on experience in the design of pile groups, the proposed approach represents a tool that can provide added-value for performance-based design and resource management, as it is very difficult, if possible at all, to develop the Pareto front based on one's experience or intuition. These potential benefits can easily outweigh the additional analysis efforts with increasing complexity in project constraints and performance requirements.

The coupled superstructure-foundation analysis approach is validated against measurements of a piled raft-supported building in London, U.K., where the superstructure layout and original pile configuration are closely modelled. Optimization analyses are then performed, and show that with the same amount of pile material, the differential settlements can be reduced by 30% by adopting the optimized pile layout. On the other hand, to achieve a performance level (differential settlements) similar to the original design, the required pile length can be reduced by 50% if an optimized layout is adopted in lieu of the original configuration.

A second case study is then presented to illustrate the effects of having a soft storey (atrium floor) on the superstructure-foundation interactions. Although the two buildings in this case only differ by the atrium floor, the resulting difference in terms of superstructure stiffness is notable. Considering the specific loading and foundation conditions, the differential settlements for the building with the atrium is approximately 2 times that of the building with shear walls on ground floor. This shows that stiffness of the upper storeys may not be effectively transferred to the foundation system when a soft storey is present. Nonetheless, this study has shown that for various cases of high-rise buildings with significant amounts of shear walls, the stiffening effects of the superstructure can be important and should be carefully considered in foundation analysis and optimization strategies.

Acknowledgements

The work presented in this paper is financially supported by the Engineering and Physical Sciences Research Council of the United Kingdom (Project No. EP/D040000/1), and the Research Grants Council of the Hong Kong Special Administrative Region (Project No. 15220415). The finite element models for the second case were constructed by Mr. Zhenxiang Su of The Hong Kong Polytechnic University. His efforts are gratefully acknowledged.

References

British Standards Institution 2008. *Eurocode 2: Design of concrete structures — Part 1-1: General rules and rules for buildings*. BSI, London, BS EN 1992-1-1:2004.

Brown, P. T. and Yu, S. K. R. 1986. "Load sequence and structure-foundation interaction." *Journal of Structural Engineering*, 112(3), 481–488.

Chamecki, S. 1956. "Structural rigidity in calculating settlements." *Journal of the Soil Mechanics and Foundation Division*, 82(SM1), 1–19.

Chan, C. M., Zhang, L. M., and Ng, J. T. M. 2009. "Optimization of pile groups using hybrid genetic algorithms." *Journal of Geotechnical and Geoenvironmental Engineering, ASCE*, 135(4), 497–505.

Chan, K. S., Karasudhi, P., and Lee, S. L. 1974. "Force at a point in the interior of a layered elastic half space." *International Journal of Solids Structures*, 10, 1179–1199.

Chow, Y. K. and Thevendran, V. 1987. "Optimisation of pile groups." *Computers and Geotechnics*, 4, 43–58.

Comodromos, E. M., Papadopoulou, M. C., and Laloui, L. 2016. "Contribution to the design methodologies of piled raft foundations under combined loadings." *Canadian Geotechnical Journal*, 53, 559–577.

Deb, K., Pratap, A., Agarwal, S., and Meyarivan, T. 2002. "A fast and elitist multi-objective genetic algorithm: NSGA-II." *IEEE Transactions on Evolutionary Computation*, 6(2), 182–197.

Guo, W. D. and Randolph, M. F. 1997. "Vertically loaded piles in non-homogeneous media." *International Journal for Numerical and Analytical Methods in Geomechanics*, 21, 507–532.

Hooper, J. A. 1973. "Observations on the behaviour of a piled-raft foundation on London clay." *Proceedings of the Institution of Civil Engineers*, 55, 855–877.

Hooper, J. A. 1979. *Review of behaviour of piled raft foundations*. CIRIA Report No. 83, Construction Industry Research and Information Association, London.

Horikoshi, K. and Randolph, M. F. 1998. "A contribution to optimum design of piled rafts." *Géotechnique*, 48(3), 301–317.

Hwang, J., Lyu, Y., and Chung, M. 2011. "Optimizing pile group design using a real genetic approach." *Proceedings of the International Offshore and Polar Engineering Conference*, 491–499.

Katzenbach, R., Arslan, U., and Moormann, C. 2000. "Piled raft foundation projects in Germany." *Design applications of raft foundations*, J. A. Hemsley, ed., Thomas Telford, 323–391.

Kim, H. T., Yoo, H. K., and Kang, I. K. 2002. "Genetic algorithm-based optimum design of piled raft foundations with model tests." *Journal of the Southeast Asian Geotechnical Society*, 33(1), 1–11.

Kim, K. N., Lee, S.-H., Kim, K.-S., Chung, C.-K., Kim, M. M., and Lee, H. S. 2001. "Optimal pile arrangement for minimizing differential settlements in piled raft foundations." *Computers and Geotechnics*, 28(4), 235 – 253.

Klar, A., Vorster, T. E. B., Soga, K., and Mair, R. J. 2007. "Elastoplastic solution for soil-pipe-tunnel interaction." *Journal of Geotechnical and Geoenvironmental Engineering, ASCE*, 133(7), 782–792.

Lavan, O. and Dargush, G. F. 2009. "Multi-objective evolutionary seismic design with passive energy dissipation systems." *Journal of Earthquake Engineering*, 13(6), 758–790.

Leung, Y. F. 2010. "Foundation optimisation and its application to pile reuse." Ph.D. thesis, University of Cambridge, United Kingdom.

Leung, Y. F., Hoult, N. A., Klar, A., and Soga, K. 2010a. "Coupled foundation-superstructure analysis and influence of building stiffness on foundation response." *Deep Foundations and Geotechnical In Situ Testing*, 61–66.

Leung, Y. F., Klar, A., and Soga, K. 2010b. "Theoretical study on pile length optimization of pile groups and piled rafts." *Journal of Geotechnical and Geoenvironmental Engineering*, 136(2), 319–330.

Leung, Y. F., Soga, K., and Klar, A. 2011. "Multi-objective foundation optimization and its application to pile reuse." *Geo-Frontiers 2011*, 75–84.

Leung, Y. F., Soga, K., Lehane, B. M., and Klar, A. 2010c. "Role of linear elasticity in pile group analysis and load test interpretation." *Journal of Geotechnical and Geoenvironmental Engineering*, 136(12).

Liu, X., Cheng, G., Wang, B., and Lin, S. 2012. "Optimum design of pile foundation by automatic grouping genetic algorithms." *ISRN Civil Engineering*, 2012.

Meyerhof, G. G. 1953. "Some recent foundation research and its application to design." *The Structural Engineer*, 31, 151–167.

Mindlin, R. D. 1936. "Force at a point in the interior of a semi-infinite solid." *Physics*, 7, 195–202.

Miyahara, F. and Ergatoudis, J. G. 1976. "Matrix analysis of structure-foundation." *Journal of the Structural Division*, 102(ST1), 251–265.

Ng, J. T. M., Chan, C. M., and Zhang, L. M. 2005. "Optimum design of pile groups in nonlinear soil using genetic algorithms." *Proceedings of the 8th International Conference on the Application of Artificial Intelligence to Civil, Structural and Environmental Engineering*, Paper 35.

Poulos, H. G. 1975. "Settlement analysis of structural foundation systems." *Proceedings of the 4th Southeast Asian Conference on Soil Engineering*, Kuala Lumpur, 4–54–4–62.

Poulos, H. G. 1979. "Settlement of single piles in nonhomogeneous soil." *Journal of the Geotechnical Engineering Division, ASCE*, 105(GT5), 627–641.

Poulos, H. G. 1989. "Pile behaviour — theory and application." *Géotechnique*, 39(3), 365–415.

Poulos, H. G. 2016. "Tall building foundations: design methods and applications." *Innovative Infrastructure Solutions*, 1(1), 1–51.

Poulos, H. G., Small, J. C., Ta, L. D., Sinha, J., and Chen, L. 1997. "Comparison of some methods for analysis of piled rafts." *Proceedings of the 14th International Conference on Soil Mechanics and Foundation Engineering*, Vol. 2, Hamburg, 1119–1124.

Reddy, M. J. and Kumar, D. N. 2007. "Multiobjective differential evolution with application to reservoir system optimization." *Journal of Computing in Civil Engineering*, 21(2), 136–146.

Reul, O. and Randolph, M. F. 2003. "Piled rafts in overconsolidated clay: comparison of in situ measurements and numerical analyses." *Géotechnique*, 53(3), 301–315.

Reul, O. and Randolph, M. F. 2004. "Design strategies for piled rafts subjected to nonuniform vertical loading." *Journal of Geotechnical and Geoenvironmental Engineering, ASCE*, 130(1), 1–13.

Small, J. C. 2001. "Practical solutions to soilstructure interaction problems." *Progress in Structural Engineering and Materials*, 3(3), 305–314.

Sommer, H. 1965. "A method for the calculation of settlements, contact pressures and bending moments in a foundation including the influence of the flexural rigidity of the superstructure." *Proceedings of the 6th International Conference on Soil Mechanics and Foundation Engineering*, Vol. 2, Montréal, 194–201.

Storn, R. and Price, K. 1997. "Differential evolution — a simple and efficient heuristic for global optimization over continuous spaces." *Journal of Global Optimization*, 11(4), 341–359.

Truman, K. Z. and Hoback, A. S. 1992. "Optimization of steel piles under rigid slab foundations using optimality criteria." *Structural Optimization*, 5, 30–36.

Valliappan, S., Tandjiria, V., and Khalili, N. 1999. "Design of raft-pile foundation using combined optimization and finite element approach." *International Journal for Numerical and Analytical Methods in Geomechanics*, 23, 1043–1065.

Weigel, T. A., Ott, K. J., and Hagerty, D. J. 1989. "Load redistribution in frame with settling footings." *Journal of Computing in Civil Engineering*, 3(1), 75–92.

Zienkiewicz, O. C. and Taylor, R. L. 2005. *The finite element method for solid and structural mechanics*. Oxford: Butterworth-Heinemann, sixth edition.

List of Figures

1 (a) Structure condensation process using finite element simulation, considering vertical load-settlement response (Leung et al. 2010a); (b) Schematic representation of piled raft model 5

2 (a) Concept of Pareto optimality in foundation optimization; (b) Calculation of crowding distance (after Deb et al., 2002) 13

3 Foundation and superstructure layout of Hyde Park Cavalry Barracks (Hooper 1973) 16

4 (a) Comparisons of settlement estimates for Hyde Park Cavalry Barracks; (b) Sensitivity analyses with different equivalent raft thickness ($\mathbf{K}^s$ not incorporated) 20

5 Comparisons of pile force estimates for Hyde Park Cavalry Barracks . . . 21

6 Optimization scheme for piled raft of Hyde Park Cavalry Barracks . . . 22

7 (a) Development of Pareto frontier using the two stage process; (b) Refined Pareto frontier with elastic-plastic analyses 24

8 Optimized pile configurations with different total pile lengths of (a) 500 m; (b) 1250 m; (c) 1500 m. Original configuration involves total pile length of 1250 m, average settlement of 17 mm and differential settlement of 14.5 mm 26

9 Bending moment estimates for (a) original pile configuration and (b) optimized pile configuration with total pile length of 1250 m 27

10 Comparisons of maximum and minimum pile forces between original and optimized pile configurations for HPCB tower 27

11 Superstructure layout for hypothetical building: (a) typical floor; (b) atrium floor. Building is symmetrical in two directions 29

12 Optimization scheme for piled raft of hypothetical building 29
13 Pareto frontiers and optimized pile configurations for buildings with and without atrium floor 31